

Morphological, Structural and Magnetic Studies of Titanium Doped Barium Ferrite

Aparna.A.R.¹, Dr.Brahmajirao.V², Dr.Kartikeyan.T.V³

¹ph.D. Research Scholar, Department Of Nanoscience and Technology, Jntu, Hyderabad, India

²Senior Professor, Dept.Of nanoscienceand Technology, Mgnirsa, Domalguda,Hyderabad

³Also: Director, Cnst, Gvpce(A), Affiliated To Jntuk, Visakhapatnam-A.P

Abstract: This paper presents the sol gel Synthesis of Ti-doped barium ferrite nanomaterial powders $\text{BaFe}_{(12-x)}\text{Ti}_x\text{O}_{19}$ for the application in magnetic coating material and nanosensors. Scifinder software couldn't trace any earlier communication involving this nanomaterial in literature. The synthesis was done:(1) at three different temperatures(850°C, 900°C and 950°C) for (x = 0.35) andfor (2) the similar nanomaterial for (x=0.33 and 0.37)at a temperature (950°C). The independent parameters chosen in our study are (i) the cited three values of 'x' and (ii) three temperatures(850°C, 900°C and 950°C).The TEM, SAED, EDS and VSM characterizations are done and the results are reported .Scifinder software couldnot trace any earlier communication

Keywords : Barium ferrite, sol-gel route, Titanium, Nano ferrites, hysteresis curve.

I. INTRODUCTION

The victims of EMI are broadband amplifiers, low level sensors, communication systems, control processors, automotive systems, weapons systems etc. Nanocomposites show efficient electromagnetic shielding response because of their unique electrical, thermal, dielectric, and magnetic properties. Conducting polymers, CNTs, graphene, dielectric titanates (Or) magnetic ferrites act as good fillers. The basic concept in the reported work is to prepare a suitable nanomaterial and characterize the same as a first step. The second step to follow the nano ferrite material is to be impregnate into intrinsic conducting polymer which will be characterized for different compositions of ingredients. The shielding effectiveness of the samples for the purpose of electromagnetic interference is done by conductance measurements and the results will appear elsewhere. Nanocomposites show efficient electromagnetic shielding response because of their unique electrical, thermal, dielectric, and magnetic properties. A wide variety of filler materials have been used for making nano composites [10] with a broad range of electrical conductivity and /electromagnetic attributes such as permittivity (ϵ) or permeability (μ). Conducting polymers, CNTs, graphene, dielectric titanates (Or) magnetic ferrites act as good fillers [11-29]. Carbon Black is most widely exploited as filler in various polymer composites [13, 21-24]. Since polymeric materials are insulating and transparent to electromagnetic energy several methods like application of conductive coatings, electro plating, vacuum metallization techniques etc., have been developed to shield plastic enclosures. Development of conducting plastic materials based on ICPs (Intrinsically conducting polymers) is promising for EMI shielding purposes [11].

The development of Nanomaterials for radar and microwave communication demands new technologies.Studies on Microwave absorbing materials for E.M.I.Shielding have increased in recent years. The main applications of these materials intend to reduce the human exposure to microwaves by means of absorbing coatings [1-3]. A suitable coating material protects the functioning of the device from being tampered by microwaves .Barium ferrite ($\text{BaFe}_{12}\text{O}_{19}$)has a very wide range of application. It is a permanent magnetic material and a ferromagnetic material. It has got better chemical stability, High saturation magnetization andgreat coercivity .It is a low cost material.useful in Microwave communication and very useful in microwave dark room[4] and also absorber for electromagnetic wave radiation.[5] .

Various studies concluded that no single material can take care of all the aspects of shield. Addition of nonmagnetic materials into barium ferrite compound will influence its sub lattice [6] and magnetic properties. In this work we have chosen Titanium-butoxide as a dopant. Because Ti-doped barium hexaferrite (Ti-doped BHF) powder is an efficient absorber of electromagnetic waves in the microwave spectrum.

II. EXPERIMENTAL METHOD

Quantities of Barium ferrite and Titanium(IV) butoxide required were evaluated stoichiometrically corresponding to the chosen value of 'x'. Weights of Barium ferrite andTitanium (IV) butoxideare measured using a 6-digit electronic microbalance. Then required amount of Citric acid (obtained earlierby dissolving solid in water of required volume) and ethyl alcohol were added. The mixture is taken in a beaker and is placed in a sonicator(containing liquid into which the beaker is placed). Ultrasonic waves are used to disperse the

ingredients of the mixture in the beaker. Then the beaker was kept on a Magnetic stirrer. Heating was done for 3hrs at 90 °C. Slowly NH₄OH was added, to moderate the pH to a value of '7', using a digital pH meter. The resulting contents of the beaker on the Magnetic stirrer is evaporated by continuous stirring to form viscous sol precursors at 80 °C & then dried at 120 °C by keeping in a oven, for 24 to 48hrs. Then the dried viscous sol was calcined for 3 hrs. At 850 °C. Same procedure is repeated for same 'x' (0.35) value by varying the temperature 900 °C and 950 °C. Again same procedure is followed by differing X (0.33 and 0.37) value and calcined at 950 °C. Final products obtained are BaFe_{11.65}Ti_{0.35}O₁₉, BaFe_{11.67}Ti_{0.33}O₁₉, and BaFe_{11.63}Ti_{0.37}O₁₉.

III. RESULTS AND DISCUSSION

1. Tem And Histogramic Analysis

TEM is an imaging technique that utilizes a high-energy beam of electrons to visualize specimens. Due to the charged nature of electrons, magnetic fields can be used to manipulate and focus the electron beam to produce structural images and diffraction patterns of materials.

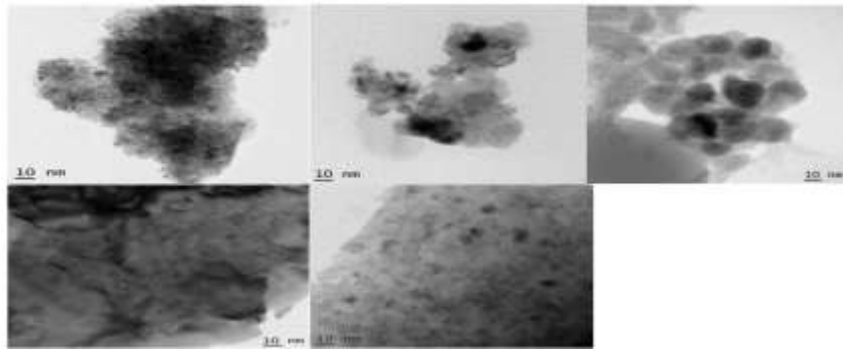
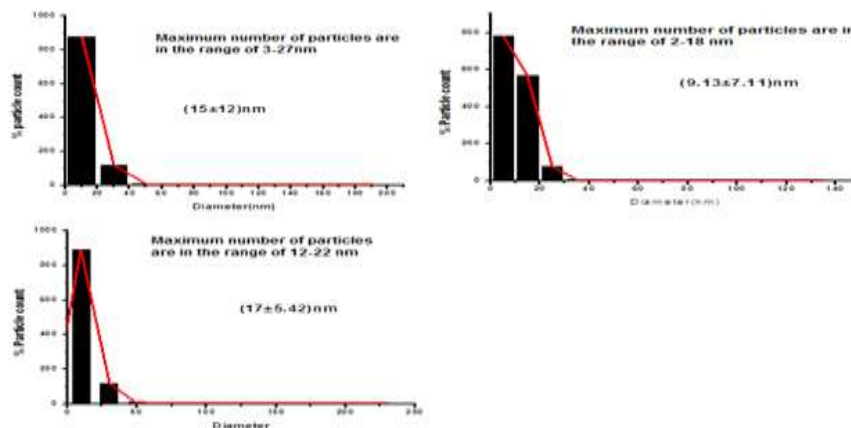


Figure 1: TEM image – (a) BaFe_{11.65}Ti_{0.35}O₁₉ (x=0.35@ 850 °C), (b) BaFe_{11.65}Ti_{0.35}O₁₉ (x=0.35@ 900 °C), (c) BaFe_{11.65}Ti_{0.35}O₁₉ (x=0.35@ 950 °C), (d) BaFe_{11.67}Ti_{0.33}O₁₉ (x=0.33@ 950 °C) and (e) BaFe_{11.63}Ti_{0.37}O₁₉ (x=0.37@ 950 °C)

The TEM and SAED data is obtained at, 'SAIF', the Indian Institute of Technology Bombay, India on a PHILIPS (Model: CM200). The TEM micrograms clearly shows that shapes are cubical. The average particle size was found to be in good agreement with the XRD data that was reported in our earlier communication [9].

Histograms were obtained by using 'image- J' software [7] on the Tem images obtained. Gaussian curve is superimposed for the statistical analysis of the data. Tabular representation brings out a comparison, of the Histograms of all five samples, (figure 2(c)) to show that the total number of particles under the Gaussian curve are very close to the expected value and that the results are in good agreement with XRD results reported by us earlier elsewhere. [9]



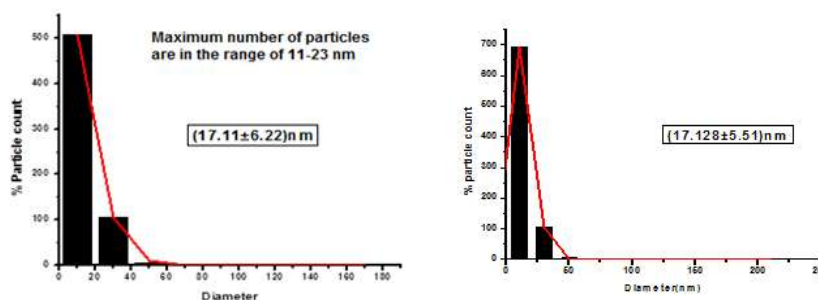


Figure 2: HISTOGRAM –(a)BaFe_{11.65}Ti_{0.35}O₁₉ (x=0.35@ 850 C),(b)BaFe_{11.65}Ti_{0.35}O₁₉ (x=0.35@ 900 C),(c)BaFe_{11.65}Ti_{0.35}O₁₉ (x=0.35@ 950 C),(d) BaFe_{11.67}Ti_{0.33}O₁₉ (x=0.33@ 950 C) and (e) BaFe_{11.63}Ti_{0.37}O₁₉ (x=0.37@ 950 C)

	(5-15)nm	(15-20)nm	Total in the three ranges
x=0.35@ 850 °C	800	100	900
x=0.35@ 900 °C	780	80	860
x=0.35@ 950 °C	900	100	1000(max)
x=0.33@ 950 °C	500	100	600(min)
x=0.37@ 950 °C	700	100	800

Saed Studies

Specific Area Electron diffraction analysis provides structural information of the sample. Often, both electron microscopy images (information in real space) and diffraction patterns (information in reciprocal space) are obtained for the same region. Electron diffraction can be performed on a single nanoparticle or an area consisting of multiple nanoparticles, by inserting the relevant selected area aperture(s)-hence the name (SAED). The SAED micrograms reveal the particle sizes in each case. They were measured at the bright spots formed due to diffraction at the corresponding particle. This was done by imaging the diffraction modes using electronwave cones over a wide energy range by the Specific Area chosen for the Electron Diffraction. Each bright dot corresponds to a displaying edge of the particle relevant to different elements locally present. These are observed for all values of X in our results. Rings are formed when atom in a crystal are systematically arranged in different miller planes. If multiple rings are formed more number of miller planes. Such a crystal is called polycrystalline. Polycrystalline structure can produce multiple number of reactions. Such a crystal gives interesting information about interactions with magnetic field, electric field, optical field etc.

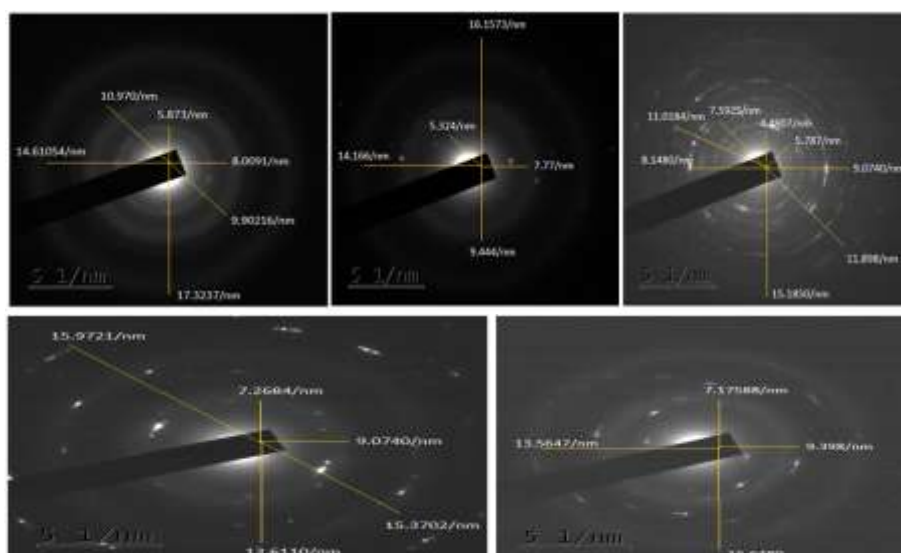


Figure 3: SAED image – (a) $\text{BaFe}_{11.65}\text{Ti}_{0.35}\text{O}_{19}$ ($x=0.35@ 850 \text{ C}$), (b) $\text{BaFe}_{11.65}\text{Ti}_{0.35}\text{O}_{19}$ ($x=0.35@ 900 \text{ C}$), (c) $\text{BaFe}_{11.65}\text{Ti}_{0.35}\text{O}_{19}$ ($x=0.35@ 950 \text{ C}$), (d) $\text{BaFe}_{11.67}\text{Ti}_{0.33}\text{O}_{19}$ ($x=0.33@ 950 \text{ C}$) and (e) $\text{BaFe}_{11.63}\text{Ti}_{0.37}\text{O}_{19}$ ($x=0.37@ 950 \text{ C}$)

Bright spots and diffraction rings are observed in all five figures 3(a,b,c,d and e). By relative comparison of these figures valuable information is revealed. Figure 3(c) has got prominent brighter spots and also prominent diffraction rings. This indicates polycrystalline nature and perfect Nano state formation in this case.

E.D.S. studies

EDS is a supplementary technique to TEM. It utilizes X-rays that are emitted from the atoms in the sample excited by the electron beam to characterize the elemental composition of the analyzed volume. Iron ions are distributed in the Nano ferrite energy wise. Fe^{2+} ions (being less energetic) occupy ‘A’ site of the spinel. Fe^{3+} ions (higher energy) occupy ‘B’ site of the spinel. Electronic conduction from ‘A’ site to ‘B’ site is caused through oxygen. EDS reveals that the dopant impurity is located both in ‘A’ as well as ‘B’ sub lattice

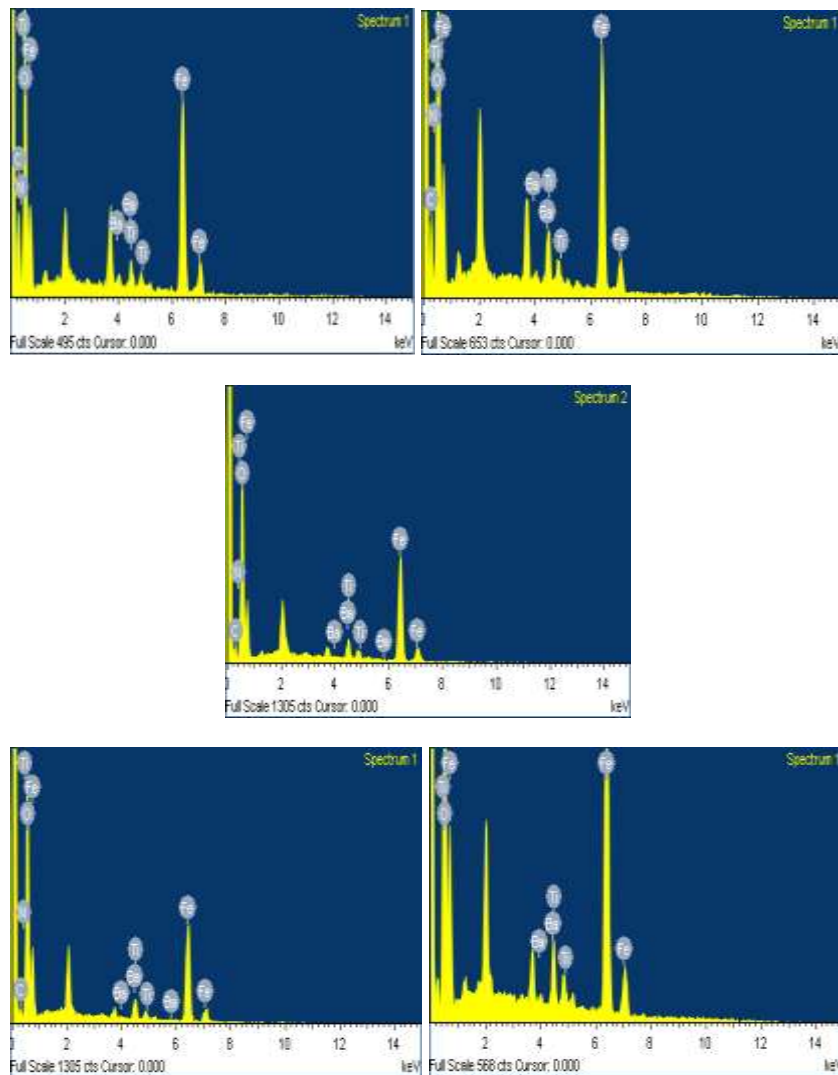


Figure 4: Edax image – (a) $\text{BaFe}_{11.65}\text{Ti}_{0.35}\text{O}_{19}$ ($x=0.35@ 850 \text{ C}$), (b) $\text{BaFe}_{11.65}\text{Ti}_{0.35}\text{O}_{19}$ ($x=0.35@ 900 \text{ C}$), (c) $\text{BaFe}_{11.65}\text{Ti}_{0.35}\text{O}_{19}$ ($x=0.35@ 950 \text{ C}$), (d) $\text{BaFe}_{11.67}\text{Ti}_{0.33}\text{O}_{19}$ ($x=0.33@ 950 \text{ C}$) and

(e) $\text{BaFe}_{11.63}\text{Ti}_{0.37}\text{O}_{19}$ ($x=0.37@ 950\text{ C}$)

The EDX data is obtained on (SEM Hitachi- S520) at Osmania University, Hyderabad, India.

The Ba peak corresponding to lower energy level (4-5Kev) is prominent for $x=0.35@ 900\text{ c}$ and less prominent for $x=0.35 @ 850\text{ c}$ and 950 c . By comparing E.D.S. plots of $x=0.35 @ 900\text{ c}$, $x=0.33$ and $x=0.37$ we can see that energy level of 4-5 Kev is more prominent for $x=0.37$. By relative comparison of peaks recorded in E.D.S. it is observed that for $x=0.35 @ 950\text{ c}$, the Ba ions are distributed in both lower level (4-5Kev) and higher level(5-6Kev). The availability of Ba at an energy value of abscissa in the EDX plot as a count of scattered x-ray photon points out the binding nature of barium ions at that energy in the lattice. However it is clear from edax spectrum that carbon and nitrogen are lying in lower energy level.

VIBRATING SAMPLE MAGNETOMETRY

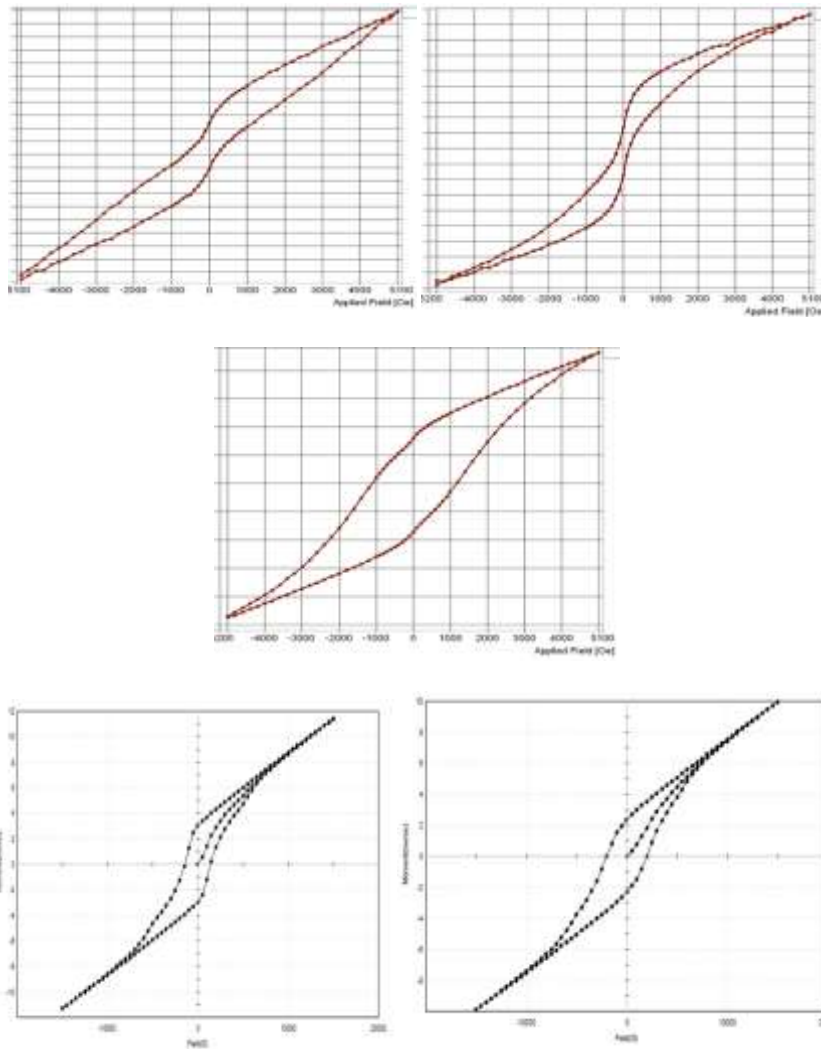


Figure 5: Hysteresis curves-(a) $\text{BaFe}_{11.65}\text{Ti}_{0.35}\text{O}_{19}$ ($x=0.35@ 850\text{ C}$), (b) $\text{BaFe}_{11.65}\text{Ti}_{0.35}\text{O}_{19}$ ($x=0.35@ 900\text{ C}$), (c) $\text{BaFe}_{11.65}\text{Ti}_{0.35}\text{O}_{19}$ ($x=0.35@ 950\text{ C}$), (d) $\text{BaFe}_{11.67}\text{Ti}_{0.33}\text{O}_{19}$ ($x=0.33@ 950\text{ C}$) and (e) $\text{BaFe}_{11.63}\text{Ti}_{0.37}\text{O}_{19}$ ($x=0.37@ 950\text{ C}$).

s.no	sample	concentration	coercivity	Retentivity (M _r)	Magnetisation (M _s)	M _r , M _s
1	BaFe _{11.65} Ti _{0.35} O ₁₉	(x=0.35@ 850°C)	394.916	0.869	5.124	0.169
2	BaFe _{11.65} Ti _{0.35} O ₁₉	(x=0.35@ 900°C)	160.296	0.768	4.366	0.173
3	BaFe _{11.65} Ti _{0.35} O ₁₉	(x=0.35@ 950°C)	1137.97	4.145	11.727	0.353
4	BaFe _{11.67} Ti _{0.33} O ₁₉	(x=0.33@ 950°C)	1433.2	2.970	11.364	0.261
5	BaFe _{11.65} Ti _{0.37} O ₁₉	(x=0.37@ 950°C)	2000.3	2.3414	9.929	0.236

When temperature is maximum (950°C) average crystallite size is minimum making the saturation magnetization maximum. This is the desirable condition is for shielding of the microwave radiation by the coating material. By relative comparison of 'x' (0.33, 0.35 and 0.37) average crystallite size is less for x=0.35 (confirmed by our earlier XRD studies [9]). Coercivity is minimum and saturation magnetization is maximum. So for this particular 'x' value Nano state formation is complete and also satisfies the desirable condition for the application of the microwave coating of the material.

Further it is interesting to note that we find the Wasp-Waist formation for the Hysteresis plots of (x=0.35@ 850 C) and (x=0.35@ 900 C). Earlier findings about such formation were reported in the paleo magnetic studies. Similar formation was reported by studies of rock formation [25]. In 1956, Meiklejohn and Bean (M-B) reported [25-27] the discovery of a new type of magnetic anisotropy called "Exchange Anisotropy". Generally Exchange anisotropy refers to the magnetic manifestations of an exchange coupling of Magnons at the interface between two different magnetically ordered systems. (Usually a ferromagnetic material and a non-ferromagnetic material).

Hysteresis loops and the demagnetization of saturation remanence [28] are parameters related to the high field magnetic behaviour of Superparamagnetic materials and the Coercivity spectra. Specific internal structures and changes in composition are found to produce characteristic effects due to them. Hysteresis loops are of three types namely (1) Single domain (2) Pseudo single domain and (3) Multi domain loops. J.S.D. Snyder [30] in his work on Magnetic Characterization of Iron Oxide Nanoparticles reported similar findings. L. Tauxe et al, [29] developed Numerical simulations to a chosen simple system (Single domain/Superparamagnetic system). The Synthetic Hysteresis loops generated by L. Tauxe et al, in a mathematical simulation revealed valuable information which in conjunction with experimental data revealed valuable information. Further analysis of the authors' findings in progress.

IV. CONCLUSION

For x=0.35@ 950 c majority of the nanoparticles formed have a diameter less than 27nm. However it is clear from EDAX spectrum that impurities are lying in lower energy level. Wasp-waist is a consequence observable in the hysteresis loop deformation. The SAED microgram recorded brighter spots and also diffraction rings. This indicates polycrystalline nature and perfect nanostate formation in this case.

ACKNOWLEDGEMENTS

Authors are thankful to the DST and the SAIF, IIT Madras for helping in FTIR analysis. Authors wish to acknowledge Dr. Moneesha Fernandes, Scientist, department of Organic chemistry, National Chemical Laboratory, Pune, India for her constant help and encouragement.

REFERENCES

- [1]. Ruan, S.-P., Xu, B.-K., Suo, H., Wu, F.-Q., Xiang, S.-Q.: J. Magn. Magn. Mater. **212**, 175–177 (2000)
- [2]. Halbedel, B., Hülsenberg, D., Belau, St., Schadewald, U.: *cfi/Ber. DKG* **82**(13), 182–188 (2005)
- [3]. Rohde & Schwarz, News 199/09, pp. 70–72 (2009)
- [4]. Li Y, Wang Q and Yang H 2009. Synthesis, characterization and magnetic properties on nanocrystalline BaFe₁₂O₁₉. *Curr. Appl. Phys.* **9** 1375-1380.
- [5]. Wang C, Han X, Xu P, Wang X, Li X and Zhao H 2009. Magnetic and dielectric properties of barium titanate-coated barium ferrite. *J. Alloy Compd.* **476** 560-565.
- [6]. Qui J, Lan L, Zhang H and Gu M 2008. Effect of titanium dioxide on microwave absorption properties of barium ferrite. *J. Alloy Compd.* **453** 261-264.

- [7]. W.Rasband, Imagej. National Institute of Health, Research Services, Branch, Bethesda, Maryland, USA (2012).
- [8]. Aparna.A.R., Dr.Brahmajirao.V, Dr.Kartikeyan.T.VandDr.MoneeshaFernandes 2016. Synthesis and Structural, Morphological & FTIR Studies on Ferrite Powders $BaFe_{(12-x)}Ti_xO_{19}$, Using Sol-Gel Method.IOSR Journal of Applied Physics (IOSR-JAP) 8.18-26.
- [9]. Aparna.A.R., Dr.Brahmajirao.Vand Dr.Kartikeyan.T.V 2016. Titanium doped barium ferrite powders ($BaFe_{(12-x)}Ti_xO_{19}$), prepared using sol gel method and characterised using XRD, SEM and FTIR techniques.IOSR Journal of Electronics and Communication Engineering (IOSR-JECE) 11.06-11.
- [10]. Praveen Sayani And Manju Arora, 2012,, Microwave Absorption and EMI Shielding Behavior of Nanocomposites Based on Intrinsically Conducting Polymers, Graphene and Carbon Nanotubes, Chapter 3,Intech Publication.
- [11]. Abbas, S.M., Aiyar, R., Prakash, O.,(1998). Synthesis and microwave absorption studies of ferrite paint. Bull Mater Sci, 21(4), 279-282.
- [12]. Pomposo, J. A., Rodríguez, J., & Grande, H. (1999). Polypyrrole-based conducting hot melt adhesives for EMI shielding applications. Synthetic Metals, 104(2), 107–111.
- [13]. Chung, D.D.L. (2001). Electromagnetic interference shielding effectiveness of carbon materials, Carbon, 39, 279- 285.
- [14]. Peng, CH., Hwang, CC., Wan, J., Tsai, J.S., Chen, SY. (2005). Microwave absorbing characteristics for composites of thermal plastic polyurethane-bonded NiZn- ferrites prepared by combustion synthesis method, Mater SciEng B, 117, 27-36.
- [15]. Jiang, J., Li, L.,& Xu, F.(2007). Polyaniline LiNi ferrite core shell composite: Preparation, characterization and properties, Mater Sci and Eng A,456, 300-304.
- [16]. Saini, P., Choudhary, V., Singh, B.P., Mathur, R.B. and Dhawan, S.K. 2011, Synth. Met., 161, 1522
- [17]. Mohammed H.Al-Saleh, Walaa H .Saadeh, UttanandaramanSundarraaj, 2013, Carbon 60, 146-156.
- [18]. Toe WookYoo, Yun Kyun Lee, SeungJoon Lim, HoGyn Yoon, Woo Nyon Kim, 2014, Journal of Material science, 49, 1701-1708.
- [19]. Hongyu Wang, Dongmei Zhu, Wancheng Zhou, and Fa Luo, Effect of Multiwalled Carbon Nanotubes on the Electromagnetic Interference Shielding Properties of Polyimide/Carbonyl Iron Composites,Ind.Eng.Chem.Res.,2015,54(25)6589-6595.
- [20]. Zhou, Li-Ying; Wu, Ming-Chun; Huang, Zhao-Xia; He, He-Zhi, AIP Conference Proceedings, Volume 1713, Issue 1, id.160001(2016).
- [21]. Gupta, A. and Choudhary, V. 2011, J. Mater. Sci., 46, 6416.
- [22]. Mathur, R.B., Singh, B.P. and Pandey, S. 2010, Polymer nanotubes nanocomposites, Synthesis properties and applications, Edited by Vikas Mittal, Wiley Scrivener, 170.
- [23]. Gogotsi, Y. 2006, Carbon Nanomaterials, CRC Press, Taylor and Francis Group.
- [24]. Abdul Khader, S., Sankarappa,T.(2015). Structural, dielectric and magnetic studies in (X) $Mn_{0.5}Zn_{0.5}Fe_2O_4 + (1-X)BaTiO_3$ magneto electricnano-composites, Int J Adv Res in PhySci, 2(8) 21-27.
- [25]. Himel Chakraborty., SumitChabri., NandagopalBhowmik. (2013). Electromagnetic interference reflectivity of nanostructured Manganese ferrite reinforced Polypyrrole composites, Transactions on Electrical and electronic materials, 14(6), 295-298.
- [26]. W.H. Meiklejohn, C.P. Bean, Phys. Rev. 102 (1956) 1413.
- [27]. W.H. Meiklejohn, C.P. Bean Phys. Rev. 105 (1957) 904.
- [28]. W.H. Meiklejohn, J. Appl. Phys. Suppl. 33 (1962) 1328.
- [29]. Stanley M. Cisowski (1980), “The relationship between the magnetic properties.....internal structure of their component Fe-oxide grains”, Geophys. J. R. astr. SOC. (1980) 60,107-122
- [30]. L. Tauxe, T.A.T.Mullender, and T.Pick (1996), “Potbellies, Wasp waists and Superparamagnetism in Magnetic Hysteresis”, J. Geophys. Res., 101(B1), pp571-583
- [31]. J.S.D.Schnyder (2010), Bachelor Thesis entitled : ‘Magnetic Characterization of Iron Oxide Nanoparticles’ submitted to ETHZurich, ZURICH